Ni^{2+}在 γ-Al_2O_3 上的分散状态及负载型 Ni/γ-Al_2O_3 催化剂的 α-蒎烯加氢活性

任世彪 邱金恒 王春燕 许波连 范以宁* 陈 懿
(南京大学化学化工学院,介观化学教育部重点实验室,江苏省纳米技术重点实验室,南京 210093)

摘要: 用 X-射线衍射(XRD)、紫外-可见漫散射光谱(UV-Vis DRS)、程序升温还原(TPR)、CO 化学吸附和微反测试等方法研究了 Ni^{2+}在 γ-Al_2O_3 上的分散状态和负载型 Ni/γ-Al_2O_3 催化剂的 α-蒎烯加氢催化活性。结果表明,当 Ni^{2+}负载量远低于其在 γ-Al_2O_3 载体表面分散容量时,Ni^{2+}优先嵌入载体表面四面体空位,随着 Ni^{2+}负载量的增加,嵌入载体表面八面体空位 Ni^{2+}的比例增大。由于八面体 Ni^{2+}易被还原为金属态 Ni^0,NiO/γ-Al_2O_3 样品的还原度随 Ni^{2+}负载量的增加而大幅度地增加,经氢还原所得 Ni/γ-Al_2O_3 催化剂的 CO 吸附量和 α-蒎烯加氢催化活性大幅度增加。对 La_2O_3 助剂的作用进行了研究,结果表明分散在 γ-Al_2O_3 上的 La^{3+}物种可阻止 Ni^{2+}嵌入 γ-Al_2O_3 表面四面体空位,增大了八面体 Ni^{2+}物种所占比例,提高了催化剂的还原度,故 Ni-La_2O_3/γ-Al_2O_3 催化剂催化活性高于 Ni/γ-Al_2O_3 催化剂。

关键词: Ni/γ-Al_2O_3; NiO/γ-Al_2O_3; 分散状态; 催化加氢; α-蒎烯
中图分类号: O643.36+1 **文献标识码**: A **文章编号**: 1001-4861(2007)06-1021-08

Dispersion State of Nickel Ions on γ-Al_2O_3 and Catalytic Activity of Derived Nickel Catalysts for Hydrogenation of α-Pinene

REN Shi-Biao QIU Jin-Heng WANG Chun-Yan XU Bo-Lian FAN Yi-Ning* CHEN Yi
(*School of Chemistry and Chemical Engineering, Nanjing University, Key Laboratory of Mesoscopic Chemistry, Ministry of Education, Jiangsu Provincal Key Laboratory of Nanotechnology, Nanjing* 210093)

Abstract: The dispersion state of nickel ions on γ-Al_2O_3 and the catalytic hydrogenation activity of supported Ni/γ-Al_2O_3 catalysts have been studied by means of X-ray diffraction (XRD), UV-Vis diffuse reflectance spectroscopy (DRS), H_2 temperature-programmed reduction (TPR), CO chemisorption and microreactor tests. It has been shown that the supported nickel ions preferentially incorporate into the tetrahedral vacancies of γ-Al_2O_3 when Ni^{2+} loading is far below its dispersion capacity on γ-Al_2O_3. Increasing Ni^{2+} loading, the ratio of Ni^{2+} ions incorporated into the octahedral vacancies of γ-Al_2O_3 increases. Since the octahedral Ni^{2+} ions are easier to be reduced to the metallic state, the reduction degree of supported NiO/γ-Al_2O_3 sample increases greatly with Ni^{2+} loading, thus resulting in a great increase in the CO uptake and catalytic activity of Ni/γ-Al_2O_3 catalyst for hydrogenation of α-pinene. The promotional effect of La_2O_3 on the catalytic activity of the supported Ni/γ-Al_2O_3 catalyst has been studied as well. It has been suggested that the dispersed La^{3+} species on γ-Al_2O_3 may inhibit incorporation of Ni^{2+} ions into the tetrahedral vacancies of γ-Al_2O_3 and increases the ratio of octahedral Ni^{2+} ions to tetrahedral Ni^{2+} ions, and thus increases the reduction degree of the catalyst precursor. As a result, the Ni-La_2O_3/γ-Al_2O_3 catalyst shows higher catalytic activity than the Ni/γ-Al_2O_3 catalyst with the same nickel loading.

Key words: NiO/γ-Al_2O_3; Ni/γ-Al_2O_3; dispersion state; α-pinene; catalytic hydrogenation

收稿日期:2007-02-14。收修改稿日期:2007-04-25。
南京大学开放测试基金资助项目。
*通讯联系人。E-mail:chem612@nju.edu.cn
第一作者:任世彪,男,33 岁,博士研究生;研究方向:多相催化。

Hydrogenation of α-pinene is one of the most important processes in fine chemical industry because of the extensive application of hydrogenation products, especially *cis*-pinane, in the synthesis of valuable fragrance compounds and drug components such as dihydromyrcenol, linalool, citronellol, citronellal, etc. Swift [1] has reviewed the hydrogenation of-pinene and the catalytic transformation of other terpenes over palladium based and nickel based catalysts. Among theses catalysts, the nickel based catalysts have been received much attention[2-8] because of their lower cost.

Metal oxide supported on γ-Al_2O_3 have been extensively studied because of their wide application as oxide catalysts and/or the precursors of supported metal and metal sulfide catalysts used in many important industrial reactions such as hydrogenation, methanation and hydrocracking. It has been well established that nickel oxide can be highly dispersed on the surface of γ-Al_2O_3 resulting in the formation of so-called "surface spinel" species, octahedral species and tetrahedral species which strongly interact with the support, and, in addition, the small crystallites of NiO will also appear on the surface when the NiO loading is high[9~18]. The amount of these nickel species depends on the loading and the temperature of calcination. In the past decades, extensive efforts have been devoted to clarify the dispersion state and reduction behavior of the supported nickel species[15~18]. Lo Jacono et al.[9] proposed that the surface spinel accommodated nickel ions in octahedral and tetrahedral sites. Wu and Hercules[14] found that the tetrahedral coordinated nickel ions are hard to be reduced, whereas octahedral nickel ions are species readily to be reduced. So far, less attention has been paid in correlating the surface structure of the support and the properties of the supported nickel species. In this work, the dispersion state and reduction behavior of Ni^{2+} on γ-Al_2O_3 were characterized by various experimental techniques and explored by the incorporation model[19] which takes into consideration the parameter of the surface structure of the support. The catalytic activity of the supported Ni/γ-Al_2O_3 catalysts derived from supported NiO/γ-Al_2O_3 samples for hydrogenation of α-pinene and the promotional effect of La_2O_3 on the catalytic activity of the supported Ni/γ-Al_2O_3 catalyst have been studied as well.

1 Experimental

1.1 Catalyst preparation

Supported NiO/γ-Al_2O_3 samples with different Ni^{2+} loadings were prepared by impregnating a γ-Al_2O_3 powder (diameter=1~2 mm, BET surface area=211 $m^2 \cdot g^{-1}$) with an aqueous solution containing nickel nitrate (Shanghai Second Chemical Reagent Factory, A.R., 0.32 $mol \cdot L^{-1}$). The NiO-La_2O_3/γ-Al_2O_3 sample with La/Ni atomic ratio of 0.3 was prepared by impregnating γ-Al_2O_3 support with an aqueous solution containing nickel nitrate (0.32 $mol \cdot L^{-1}$) and lanthanum nitrate (Shanghai Second Chemical Reagent Factory, A.R., 0.10 $mol \cdot L^{-1}$), dried at 120 ℃ overnight and calcined at 550 ℃ in air for 5 h. All the samples were reduced at 500 ℃ in H_2 flow of 30 $mL \cdot min^{-1}$ for 4 h before catalytic evaluation and CO chemisorption.

1.2 X-ray diffraction (XRD) measurement

XRD patterns were obtained by using a Shimadzu XD-3A diffractometer with a Ni-filtered Cu *K*α-radiation(λ=0.154 18 nm) at 40 kV and 40 mA. The amount of bulk NiO was determined by XRD quantitative analysis using α-Al_2O_3 powder as a reference [20,21]. The diffraction peak intensity ratio of NiO(200) plane to α-Al_2O_3(116) plane (denoted as $I_{NiO}/I_{\alpha-Al_2O_3}$) in the NiO/$\gamma$-$Al_2O_3$ samples with different Ni^{2+} loadings were measured, from which the dispersion capacity of NiO on γ-Al_2O_3 was evaluated.

1.3 UV-Vis diffuse reflectance spectroscopy (DRS)

UV-Vis DRS were recorded in the range of 190~900 nm by a Shimadzu UV-2401 PC spectrophotometer using γ-Al_2O_3 as a reference.

1.4 Hydrogenation of α-pinene

Hydrogenation of α-pinene was carried out in a fixed-bed mircoreactor with a tubular stainless reactor (45 cm length, 35 mm o.d. and 30 mm i.d.) under reaction conditions of 170 ℃, 0.1 MPa, H_2/α-pinene molar ratio=80 and liquid (*V*/*V*) hour space velocity (LHSV)=0.4 h^{-1}(α-pinene). The reaction products were analyzed by an online gas chromatograph system with

an OV-1701 capillary column (30 m ×0.25 mm × 0.33 μm)and a flame ionization detector. The column temperature was first held at 75 ℃ for 5 min and then raised to 220 ℃ with a rate of 10 ℃·min^{-1} and held at 220 ℃ for 20 min.

1.5 Temperature-programmed reduction (TPR)

Temperature-programmed reduction (TPR) was carried out in a quartz U-tube reactor with an inner diameter of 6 mm and 100 mg sample for each measurement. The samples were heated from room temperature to 900 ℃ at a ramp of 5 ℃·min^{-1} in a H_2-Ar mixture (5% H_2 by volume) with a flow rate of 40 mL·min^{-1}. The consumption of H_2 was detected by a thermal conductive detector. The reduction degree of different pre-reduced NiO/γ-Al_2O_3 samples at 500 ℃ in H_2 for 4 h were also evaluated by TPR measurements and denoted as $Rd=(A_b-A_a)/A_b\times100\%$, in which A_b and A_a are the H_2 consumption peak areas in the TPR profiles before and after pre-reduction of the samples under the above conditions, respectively.

1.6 CO chemisorption

CO chemisorption on the pre-reduced samples was carried out in a Micromertics ASAP2020C instrument using a conventional static method. All the samples were first reduced at 500 ℃ in H_2 flow and then outgassed at the same temperature for 1 h. The CO uptake was measured at room temperature, and the dispersion of metallic Ni (D, %) and the average particle size of metallic Ni (d, nm) in the pre-reduced samples were calculated assuming a CO/Ni^0 ratio of 1.0[22-24].

2 Results and discussion

XRD patterns of NiO/γ-Al_2O_3 samples with different Ni^{2+} loadings are shown in Fig.1. One can see only the characteristic peaks of γ-Al_2O_3 in the samples with Ni^{2+} loading less than 1.275 mmol Ni^{2+}/100 m^2 γ-Al_2O_3 (Fig.1b~f). And, in contrast, both the characteristic peaks of NiO (2θ=37.3°, 43.3° and 62.9°) and γ-Al_2O_3 can be seen in the mechanical mixture with the same composition (Fig.1c′), suggesting that the Ni^{2+} ions are highly dispersed in NiO/γ-Al_2O_3 samples with Ni^{2+} loading less than 1.275 mmol Ni^{2+}/100 m^2 γ-Al_2O_3. Beyond this value the characteristic peaks attributed to NiO crystallite are observed in the XRD patterns of the samples (Fig.1g~j). Plotted in Fig.2 are the ratios of the XRD peak intensities of NiO (200) to α-Al_2O_3 (116) reference versus the loading amounts of Ni^{2+} in these samples, from which the dispersion capacity of Ni^{2+} on γ-Al_2O_3 is determined to be 1.270 mmol Ni^{2+}/100 m^2 γ-Al_2O_3 by extrapolation. This value is lower than that previously reported elsewhere (1.50 mmol Ni^{2+}/100 m^2 γ-Al_2O_3)[19], probably because of the different γ-Al_2O_3 support used.

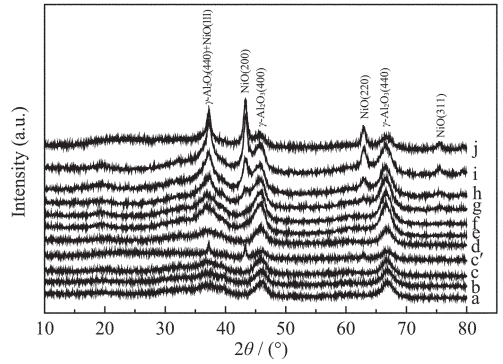

(a) γ-Al_2O_3; (b) 0.170; (c) 0.255; (c′) 0.255, (NiO + γ-Al_2O_3) mechanical mixture; (d) 0.425; (e) 0.595; (f) 0.850; (g) 1.275; (h) 1.700; (i) 2.125; (j) 2.975

Fig.1 XRD patterns of NiO/γ-Al_2O_3 samples with different Ni^{2+} loading (mmol Ni^{2+}/100 m^2 γ-Al_2O_3)

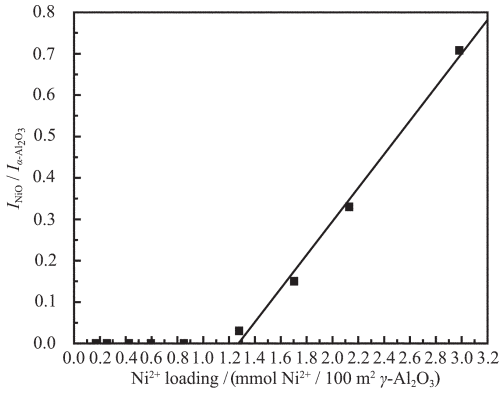

Fig. 2 XRD quantitative analysis result of NiO/γ-Al_2O_3

Shown in Fig.3 are the UV-Vis diffuse reflectance spectra of NiO/γ-Al_2O_3 samples with different loadings. For the samples with Ni^{2+} loadings far lower than the dispersion capacity of Ni^{2+} on γ-Al_2O_3, the absorption bands are observed (Fig.3b, c) at 590 and 635 nm attributed to the absorption of Ni^{2+} ions incorporated into the tetrahedral vacancies in the sur-

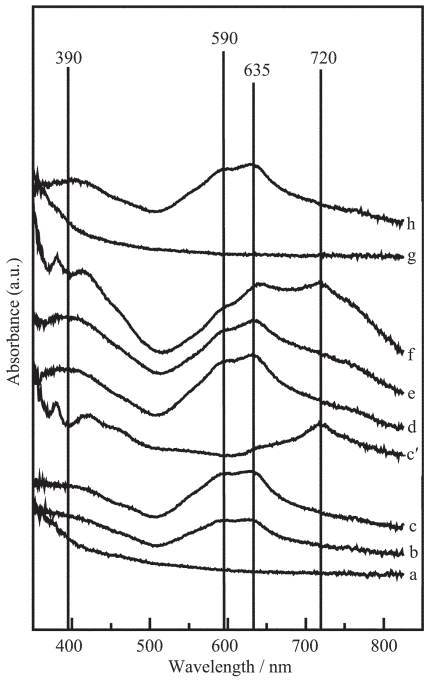

(a) γ-Al_2O_3; (b) 0.170; (c) 0.255; (c′) 0.255, (NiO+γ-Al_2O_3) mechanical mixture; (d) 0.425; (e) 0.595; (f) 1.70; (g) La_2O_3/γ-Al_2O_3 (0.255 mmol La^{3+}/100 m^2 γ-Al_2O_3); (h) NiO-La_2O_3/γ-Al_2O_3 (0.255 mmol Ni^{2+}/100 m^2 γ-Al_2O_3, 0.076 mmol La^{3+}/100 m^2 γ-Al_2O_3, La/Ni atomic ratio=0.3).

Fig.3 UV-Vis DRS spectra of NiO/γ-Al_2O_3 samples with different NiO loadings (mmol Ni^{2+}/100 m^2 γ-Al_2O_3)

face of γ-Al_2O_3[9,10]. With increasing Ni^{2+} loading, a broad absorption band in vicinity of 390 nm appears and its intensity increases with increasing Ni^{2+} loading (Fig.3d, e). This band is ascribed to the absorption of Ni^{2+} ions incorporated into the octahedral vacancies in the surface of γ-Al_2O_3[9,10,25]. These results indicate that Ni^{2+} ions preferentially incorporate into the tetrahedral vacancies of γ-Al_2O_3. With increasing Ni^{2+} loading, the ratio of Ni^{2+} ions incorporated into the octahedral vacancies of γ-Al_2O_3 increases. For the samples with Ni^{2+} loading higher than the dispersion capacity of Ni^{2+} on γ-Al_2O_3 (Fig.3f), the excess Ni^{2+} exists in the NiO crystalline form, as the absorption band at 720 nm attributed to the absorption of the crystalline NiO[25] can be observed. This is consistent with the above XRD results.

To discuss the interactions between the dispersed oxide species and an oxide support, the surface structure of the support should be taken into consideration. As suggested by incorporation model[19], the dispersed metal cations might incorporate into the vacant sites available on the surface of the support with the accompanied anions as capping anions for charge compensation. It has been well established that γ-Al_2O_3 has a spinel structure with its (110) plane preferentially exposed on the surface[26] as shown in Fig.4. The structure of γ-Al_2O_3 consists of particles formed by one dimensional stacking of C-and D-layers, and the exposure possibilities of these two layers are equal[26]. The distribution of Al^{3+} per unit mesh (0.443 nm^2, based on 0.14 nm radius of the O^{2-} ion[27]) can be expressed as $[Al_2O_4]$ for the D-layer, and as $Al_{4/3}{}^*{}_{2/3}[Al_2O_4]$ for C-layer, where * denotes the vacancies due to the defect spinel structure of γ-Al_2O_3. On the preferentially exposed (110) plane of γ-Al_2O_3 there are two kinds of surface vacant sites, i. e., octahedral and te-

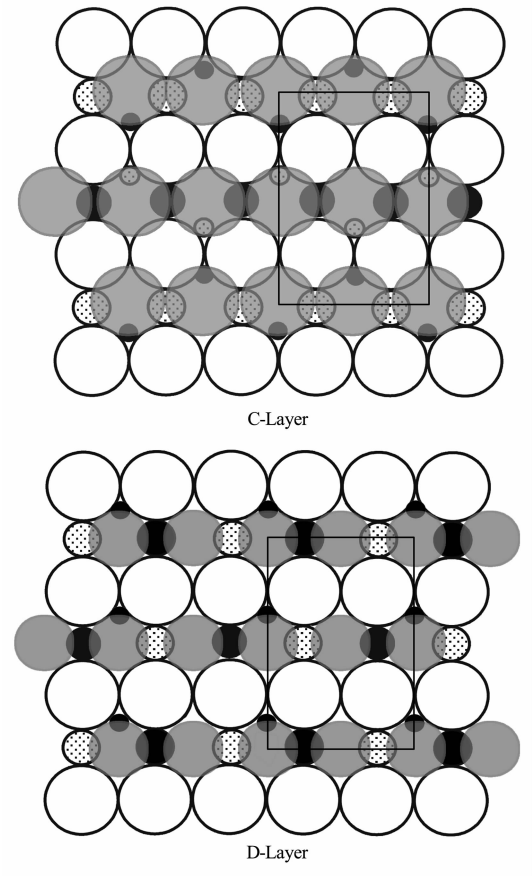

Fig.4 Schematic diagram for the incorporated Ni^{2+} ions in the surface vacant sites of the (110) plane of γ-Al_2O_3

trahedral sites. The incorporation of Ni^{2+} ions into some of the exposed vacant sites is assumed to result in the formation of octahedral or tetrahedral Ni^{2+} ions. In order to compensate the extra positive charge, an oxygen anion associated with the Ni^{2+} ion will stay at the top of the occupied site as a capping oxygen. As a consequence of the shielding effect of the capping oxygen anions, only part of the available vacant sites are usable. Thus at most 4 Ni^{2+} ions can be implanted in a unit mesh of D layer, and $4-4\frac{2}{3}$ Ni^{2+} ions in a unit mesh of C layer, where the value of $\frac{2}{3}$ comes from consideration of Al^{3+}(Tet.) vacancies. The capping oxygen anions formed an epitaxial layer on the top of the γ-Al_2O_3 surface, as shown in Fig.4. Then the dispersion capacity of nickel ions on γ-Al_2O_3 is estimated to be 9.0~9.8 nm^{-2} (1.50~1.63 mmol Ni^{2+}/100 m^2 γ-Al_2O_3). The value is very close to the experimentally measured dispersion capacity of nickel ions (1.270 mmol Ni^{2+}/100 m^2 γ-Al_2O_3) mentioned above, suggesting that the dispersed nickel ions might locate on the vacant site in γ-Al_2O_3 with the accompanied oxygen anions positioning on the top as shown schematically in Fig.4.

Table 1 shows the catalytic properties of supported Ni/γ-Al_2O_3 catalysts for hydrogenation of α-pinene at steady state (reaction for ca. 6.5 h). The main products of the catalytic hydrogenation of α-pinene on the supported Ni/γ-Al_2O_3 catalyst are *cis*-pinane and trans-pinane. It can be seen from Table 1 that the catalytic activity of Ni/γ-Al_2O_3 catalyst for hydrogenation of α-pinene remarkably increases with increasing Ni^{2+} loading. Noteworthily, the relative catalytic activity (denoted as α-pinene conversion per unit Ni weight in the catalysts) of Ni/γ-Al_2O_3 catalyst first increases greatly and then decreases slightly with increasing Ni^{2+} loading as shown in Fig.5. The decrease in relative activity may be correlated to the decrease of metallic nickel dispersion due to the increase of Ni loading. However, the much lower relative catalytic activity of Ni/γ-Al_2O_3 catalyst with Ni^{2+} loading far below its dispersion capacity or the great increase of relative activity with increasing Ni^{2+} loading can not be explained merely by different nickel content in the catalyst. For the catalytic activity of Ni/γ-Al_2O_3 catalyst derived from the NiO/γ-Al_2O_3 sample with Ni^{2+} loading far below its dispersion capacity, the interaction of Ni^{2+} with γ-Al_2O_3 support and the state of nickel species in the pre-reduced catalysts should be taken into consideration.

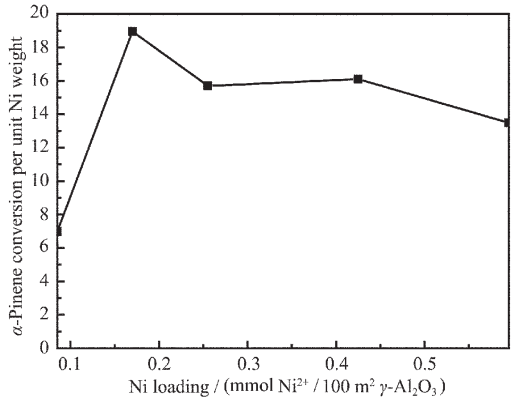

Fig.5　Relative activities of Ni/γ-Al_2O_3 catalysts with different Ni loadings

Table 1　Catalytic properties of supported Ni/γ-Al_2O_3 catalysts

Catalyst	Ni Loading		α-Pinene conversion	Selectivity / (mol%)		Relative
	/ (mmol Ni / 100 m^2 γ-Al_2O_3)	/ (wt%)	/ (mol%)	*cis*-Pinane	*trans*-Pinane	activity [a]
Ni/γ-Al_2O_3	0.085	1.0	7.0	63.0	37.0	7.0
	0.170	2.0	37.9	86.5	13.5	19.0
	0.255	3.0	47.1	90.5	9.5	15.7
	0.425	5.0	80.5	84.5	15.5	16.1
	0.595	7.0	94.5	79.2	20.8	13.5
Ni-La_2O_3/γ-Al_2O_3 (La/Ni=0.3)	0.255	3.0	77.8	85.1	14.9	25.9

[a] represents α-pinene conversion per unit Ni weight for the catalyst concerned

TPR results of a series of samples are shown in Fig.6. As shown by profile 6a~d, no H_2 consumption under 500 ℃ can be observed for NiO/γ-Al_2O_3 with Ni^{2+} loading lower than its dispersion capacity, and in contrast, profile 6b′ for the mechanical mixture of NiO with γ-Al_2O_3 has a reduction peak corresponding to the reduction of Ni^{2+} to metallic Ni^0 located at 350 ℃. This result indicates that the supported Ni^{2+} ions are well dispersed on γ-Al_2O_3 support and the dispersed Ni^{2+} ions are difficult to reduce due to strong interaction between Ni^{2+} and γ-Al_2O_3 support. For the samples with Ni^{2+} loadings far lower than the dispersion capacity of Ni^{2+} on γ-Al_2O_3, only H_2 consumption peak at ca. 810 ℃ attributed to reduction of the Ni^{2+} ions incorporated into tetrahedral vacancies in the surface of γ-Al_2O_3[14,28] can be observed (profile 6a, b). With increasing Ni^{2+} loading, a new H_2 consumption peak appears with an increased intensity at ca. 680℃ attributed to reduction of the Ni^{2+} ions incorporated into octahedral vacancies in the surface of γ-Al_2O_3 [14,28] (profile 6c, d). These results are in good agreement with the results of UV-Vis DRS, suggesting that dispersed Ni^{2+} ions incorporate into the octahedral vacancies and tetrahedral vacancies of γ-Al_2O_3. When Ni^{2+} loading is far lower than its dispersion capacity, the dispersed Ni^{2+} ions preferentially incorporate into the tetrahedral vacancies of γ-Al_2O_3 to form tetrahedral Ni^{2+} ions. With increasing Ni^{2+} loading, the ratio of octahedral Ni^{2+} species to tetrahedral Ni^{2+} species increases greatly.

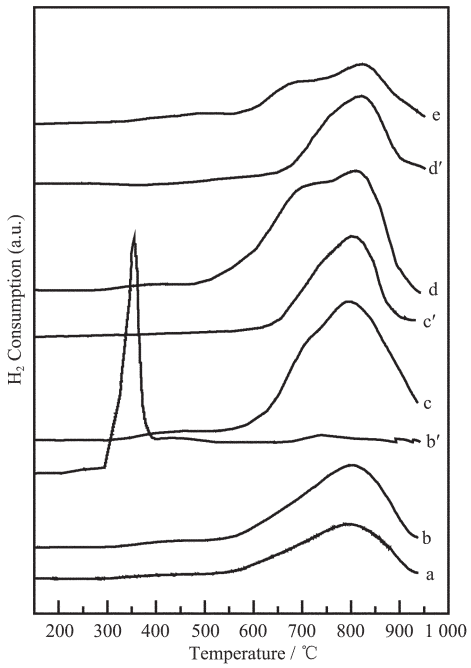

(a) 0.170; (b) 0.255; (b′) 0.255, (NiO + γ-Al_2O_3) mechanical mixture; (c) 0.425; (c′) c sample pre-reduced at 500 ℃ in H_2 for 4 h; (d) 0.595; (d′) d sample pre-reduced at 500 ℃ in H_2 for 4 h; (e) NiO-La_2O_3/γ-Al_2O_3 (0.255 mmol Ni^{2+}/100 m^2 γ-Al_2O_3, 0.076 mmol La^{3+}/100 m^2 γ-Al_2O_3, La/Ni atomic ratio=0.3)

Fig.6 TPR profiles of NiO/γ-Al_2O_3 samples with different Ni^{2+} loadings (mmol Ni^{2+}/100 m^2 γ-Al_2O_3)

After the samples being pre-reduced under pure H_2 at 500 ℃ for 4 h, the H_2 consumption peaks in the profiles (6c′, 6d′) corresponding to the reduction of tetrahedral Ni^{2+} can be observed. This result indicates that the octahedral Ni^{2+} species on γ-Al_2O_3 support can be reduced to metallic nickel (Ni^0), while the tetrahedral Ni^{2+} species exist in its oxidized state after the samples being treated under the above conditions.

As shown in Table 2 the reduction degree increases greatly with Ni^{2+} loading. As discussed above, the dispersed Ni^{2+} ions preferentially incorporate into the tetrahedral vacancies of γ-Al_2O_3 to form tetrahedral

Table 2 Reduction degree and CO uptake of supported Ni/γ-Al_2O_3 catalysts

Catalyst	Ni loading / (mmol Ni / 100 m^2 γ-Al_2O_3)	Ni loading / (wt%)	Rd / (%)	CO uptake / (mL / g Ni)	*D* / %	*d* / nm
Ni/γ-Al_2O_3	0.085	1.0	0.9	1.4	56.1	1.9
	0.170	2.0	3.5	4.1	47.6	2.4
	0.255	3.0	7.2	12.2	42.6	2.8
	0.425	5.0	27.0	38.0	40.2	3.4
	0.595	7.0	55.2	79.3	37.6	3.8
Ni-La_2O_3/γ-Al_2O_3 (La/Ni=0.3)	0.255	3.0	25.0	32.5	38.4	3.2

Ni^{2+} ions, and a ratio of octahedral Ni^{2+} species to tetrahedral Ni^{2+} species increases with Ni^{2+} loading. As the octahedral Ni^{2+} ions are easier to be reduced than the tetrahedral Ni^{2+} ions, the reduction degree and CO chemisorption uptake increase greatly with Ni^{2+} loading. These results lead to the argument that much lower relative catalytic activity of Ni/γ-Al_2O_3 catalyst derived from the NiO/γ-Al_2O_3 sample with Ni^{2+} loading far lower than its dispersion capacity is correlated to lower reduction degree and lower content of metallic Ni^0 in the catalysts.

As shown in Table 1, by doping La_2O_3 component to the supported Ni/γ-Al_2O_3 catalyst, α-pinene conversion and the relative catalytic activity of Ni-La_2O_3/γ-Al_2O_3 catalyst increase remarkably, indicating that La_2O_3 component has a promotional effect on the supported Ni/γ-Al_2O_3 catalyst for hydrogenation of α-pinene. Similar promotional effect has also been found in the supported Ni-La_2O_3/γ-Al_2O_3 catalysts for the reforming of methane with carbon dioxide[29] and for the partial oxidation of methane to carbon monoxide and hydrogen[30]. Chu et al.[30] correlated this promotional effect to the easier reduction of oxidized nickel species in the Ni-La_2O_3/γ-Al_2O_3 catalysts. However, the promotional effect of La_2O_3 on the reduction of oxidized nickel species in the Ni-La_2O_3/γ-Al_2O_3 catalyst is still unclear. In our cases, it can be seen from Fig.7 that only the characteristic peaks of γ-Al_2O_3 in the NiO-La_2O_3/γ-Al_2O_3 sample (Fig.7b). In contrast, the characteristic peaks of both NiO (2θ=37.3°, 43.3° and 62.9°) and $La(OH)_3$ (2θ=27.4°, 28.0° and 39.6°) can be seen in the mechanical mixtures of the same composition (Fig.1c′, Fig.7d), suggesting that both Ni^{2+} and La^{3+} species are highly dispersed in the supported NiO-La_2O_3/γ-Al_2O_3 sample. Interestingly, the dispersed La^{3+} species result in the increase of the ratio of octahedral Ni^{2+} ions to tetrahedral Ni^{2+} ions, as the absorption band at 390 nm are more intense (Fig.3h) than that of NiO/γ-Al_2O_3 sample (Fig.3c). Accordingly, the H_2 consumption peak intensity at ca. 680 ℃ attributed to the reduction of the octahedral Ni^{2+} ions increases obviously, while the H_2 consumption peak intensity at ca. 810 ℃ attributed to the reduction of the tetrahedral Ni^{2+} ions decreases (Fig.6e). With increasing the ratio of octahedral Ni^{2+} species to tetrahedral Ni^{2+} species in the NiO-La_2O_3/γ-Al_2O_3 sample, reduction degree (Rd) and CO uptake increase greatly as shown in Table 2. Based on the above results and discussion, one can conclude that the dispersed La^{3+} species may inhibit the incorporation of Ni^{2+} ions into tetrahedral vacancies in the surface of γ-Al_2O_3 support and increases the ratio of Ni^{2+} ions incorporated into the octahedral vacancies of γ-Al_2O_3. Because the octahedral Ni^{2+} ions are easier to be reduced to the metallic state, which can act as the catalytically active component for hydrogenation of α-pinene, the Ni-La_2O_3/γ-Al_2O_3 catalyst shows higher catalytic activity for hydrogenation of α-pinene than the Ni/γ-Al_2O_3 catalyst with the same Ni loading.

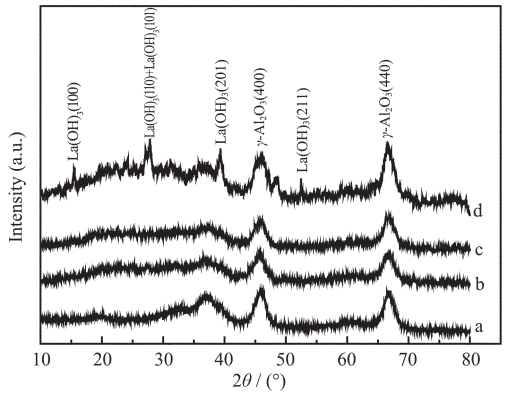

(a) NiO/γ-Al_2O_3(0.255 mmol Ni^{2+}/100 m^2 γ-Al_2O_3);
(b) NiO-La_2O_3/γ-Al_2O_3 (0.255 mmol Ni^{2+}/100 m^2 γ-Al_2O_3, 0.076 mmol La^{3+}/100 m^2 γ-Al_2O_3, La/Ni atomic ratio=0.3);
(c) La_2O_3/γ-Al_2O_3 (0.255 mmol La^{3+}/100 m^2 γ-Al_2O_3);
(d) (La_2O_3+γ-Al_2O_3) mechanical mixture (0.255 mmol La^{3+}/100 m^2 γ-Al_2O_3)

Fig.7　XRD patterns of NiO-La_2O_3/γ-Al_2O_3 samples

3　Conclusions

(1) The experimentally measured dispersion capacity of Ni^{2+} on γ-Al_2O_3 by XRD is close to the dispersion capacity expected by incorporation model. The results seem to suggest that in the NiO/γ-Al_2O_3 samples the highly dispersed nickel ions are positioned on the surface vacant sites of the γ-Al_2O_3 support.

(2) When the Ni^{2+} loading is far below its dispersion capacity on γ-Al_2O_3, the supported nickel ions preferentially incorporated into the tetrahedral vacan-

cies of γ-Al_2O_3. Increasing Ni^{2+} loading, the ratio of Ni^{2+} ions incorporated into the octahedral vacancies of γ-Al_2O_3 increases. As the octahedral Ni^{2+} ions are easier to be reduced to the metallic state, reduction degree of the supported NiO/γ-Al_2O_3 sample increases, leading to a great increase in the CO uptake and catalytic activity of Ni/γ-Al_2O_3 catalyst for hydrogenation of α-pinene.

(3) The dispersed La^{3+} species on γ-Al_2O_3 increases the ratio of octahedral Ni^{2+} ions to tetrahedral Ni^{2+} ions, and thus increases the reduction degree of catalyst precursor. As a result, the Ni-La_2O_3/γ-Al_2O_3 catalyst shows higher catalytic activity than the Ni/γ-Al_2O_3 catalyst with the same nickel loading.

References:

[1] Swift K A D. *Top. Catal.*, **2004**,**27**:143~155

[2] Fisher G S, Stinson J S, Goldblatt L A, et al. *J. Am. Chem. Soc.*, **1953**,**75**:3675~3678

[3] Ko S H, Chou T C. *Ind. Eng. Chem. Res.*, **1993**,**32**:1579~1587

[4] Ko S H, Chou T C. *Ind. Eng. Chem. Res.*, **1995**,**34**:457~467

[5] Ko S H, Chou T C. *Can. J. Chem. Eng.*, **1994**,**72**:862~873

[6] Cocker W, Shannon P V R, Staniland P A, et al. *J. Chem. Soc. C*, **1966**,**4**:1~47

[7] Bazhenov Y P, Kasyanova L Z, Bokin A I, et al. *Russ. J. Appl. Chem.*, **2003**,**76**:234~237

[8] YU Xiao-Bing(余小兵), TAN Xie-Feng(谈燮峰), XIAO Shu-De(萧树德), et al. *Guangzhou Huaxue*(*Chinese Guangzhou Chem.*), **1999**,**3**:20~24

[9] Jacono M L, Schiavello M, Cimino A, et al. *J. Phys. Chem.*, **1971**,**75**:1044~1050

[10]Burggraf L W, Leyden D E. *J. Catal.*, **1982**,**78**:360~379

[11]Scheffer B, Heijeinga J J, Moulijn J A, et al. *J. Phys. Chem.*, **1987**,**91**:4752~4759.

[12]Ho S C, Chou T C. *Ind. Eng. Chem. Res.*, **1995**,**34**:2279~2284.

[13]Cai X H, Ren Z G, Xie Y C, et al. *Surf. Interface Anal.*, **2001**, **32**:293~295

[14]Wu M, Hercules D M. *J. Phys. Chem.*, **1979**,**83**:2003~2008

[15]Li G H, Hu L J, Hill J M, et al. *Appl. Catal. A*: *General.* **2006**,**301**:16~24

[16]Wang S B, Lu G Q. *Appl. Catal. A*: *General*. **1998**,**169**:271~280

[17]Heracleous E, Lee A F, Lemonidou, A A. *J. Catal.*, **2005**, **231**:159~171

[18]Scheffer B, Molhoek P, Moulijn J A, et al. *Appl. Catal. A*: *General*, **1989**,**46**:11~30

[19]Chen Y, Zhang L F. *Catal. Lett.*, **1992**,**12**:51~62

[20]XU Bo-Lian(许波连), FAN Yi-Ning(范以宁), CHEN Yi(陈 懿), et al. *Zhongguo Kexue B* (*Sci. China Ser. B*), **2002**,**45**:407~415

[21]Xie Y C, Tang Y Q. *Adv. Catal.*, **1990**,**37**:1~43

[22]Choudhary T V, Sivadinarayana C, Goodman D W, et al. *Catal. Lett.*, **2001**,**72**:197~201

[23]Yin S F, Zhang Q H, Xu B Q, et al. *J. Catal.*, **2004**,**224**: 384~396

[24]Cheng D G, Zhu X L, Liu C J, et al. *Catal. Today*, **2006**,**115**: 205~210

[25]Wang J, Dong L, Hu Y H, et al. *J. Solid State Chem.*, **2001**, **157**:274~282

[26]Schuit G C A, Gates B C. *AIChE J.*, **1973**,**19**:417~38

[27]DONG Lin(董 林), CHEN Yi(陈 懿). *Wuji Huaxue Xuebao*(*Chinese J. Inorg. Chem.*), **2000**,**16**:250~260

[28]Zhang L F, Lin J F, Chen Y J, et al. *J. Chem. Soc. Faraday Trans.*, **1992**,**88**:497~503

[29]Cheng Z X, Wu Q L, Zhu Q M, et al. *Catal. Today*, **1996**, **30**:147~155

[30]Chu Y L, Li S B, Lin J Z, et al. *Appl. Catal. A*: *General*, **1996**,**134**:67~80